



Characterization of chitin and description of its antimicrobial properties obtained from *Cydalima perspectalis* adults

Leyla Kılıcı¹ · Nurver Altun¹ · Şengül Alpay Karaoğlu¹ ·
Tuğçe Karaduman Yeşildal^{1,2}

Received: 20 April 2023 / Revised: 22 August 2023 / Accepted: 24 June 2024
© The Author(s) 2024

Abstract

Chitin is the most abundant biopolymer group after cellulose and forms the exoskeleton of arthropods, the largest animal group. The morphology of chitin differs between and within species. In this study, we determined the physicochemical and biological activity of chitin samples obtained from different body parts of the boxwood moth *Cydalima perspectalis* for its application as a biotechnological material. The collected chitin samples were characterized by scanning electron microscopy (SEM), Fourier-transform infrared spectroscopy (FTIR), thermogravimetric analysis (TGA), and elemental analysis. FTIR confirms that the isolation of chitin is successful. The SEM results showed that the surface morphology of the obtained chitins was both fibrous and porous and had a rough surface. As a result of the elemental analysis, the %N values of chitins were calculated as 6.60 on average, and the values were shown to be close to each other. We also investigated the biocompatibility and antimicrobial properties of these chitin samples. We used L929 (mouse fibroblast) cells to perform indirect cytotoxicity experiments and investigated their viability by performing the MTT assay. Our findings showed that the samples had no cytotoxic effect on the L929 cells at 24, 48, and 72 h. The cytotoxic study showed that *Escherichia coli*, *Bacillus subtilis*, *Staphylococcus aureus* bacteria, and *Candida albicans* fungi adhered to chitin surfaces regarding biofilm production. The chitin contents were determined as 21.02% for the head, 5.74% for the body, 32.22% for the wing, 33.53% for the legs, and 2.65% for the pupal shell. Chitin is a material with high potential for use in various fields. Our findings suggested that *Cydalima perspectalis* can be used as an alternative source of chitin in biomedical applications.

✉ Nurver Altun
nurver.altun@erdogan.edu.tr

¹ Department of Biology, Faculty of Arts and Sciences, Recep Tayyip Erdogan University, Fener Mah., Rize 53100, Turkey

² Department of Molecular Biology and Genetics, Faculty of Science and Letters, Aksaray University, Aksaray, 68100, Turkey

Keywords Lepidoptera · Chitin · Characterization · *Cydalima perspectalis*

Introduction

Chitin ($C_8H_{13}O_5N$)_n is a polysaccharide consisting of *N*-acetyl-D-glucosamine groups. It is the most abundant biopolymer in the world after cellulose. It has a long-chain biopolymer structure and regular crystalline microfibrils [1]. Chitin is found in the fungal cell wall, the exoskeleton of arthropods, and the basic shell structure of marine crustaceans [2]. Chitins have been characterized by sponges [3, 4], anthozoans [5], and even the feet of chickens [6]. Particularly insects and crustaceans are rich in chitin content. Insects are one of the essential sources of chitin after crustaceans [7–9]. The structural features of the insect exoskeleton are a subject that continues to be investigated [10]. The cuticle on the outer wall of insects is mainly composed of protein, chitin and lipid. Chitin makes up about 30% of the cuticle. According to data from many insects, chitins are composed of microfibrils with a diameter of about 2.8 nm and helically arranged in layers [11]. Chitin samples from different organisms may differ in their physicochemical properties [12, 13]. Chitin is biocompatible, biodegradable, antitumorigenic, and antimicrobial, and thus, might be used in areas where hygiene is essential, such as in textile, food, agriculture, medicine, and pharmacy [14]. Therefore, the demand for chitin derived from insect cuticles as a biomaterial is relatively high [15]. Studies in the literature are conducted with different insect groups to produce and characterize chitin. Chitin was extracted from housefly (*Musca domestica*), silkworm (*Bombyx mori*) pupa exuvia, *Melolontha melolontha*, *Calliptamus barbarus*, *Oedaleus decorus*, beetle (*Holotrichia parallela*), bumblebee (*Bombus terrestris*), *Lucanus cervus*, *Polyphylla fullo*, butterfly (*Argynnis pandora*), *Hermetia illucens* and *Vespa crabro* (wasp) [16–24]. Chitin occurs in three different forms depending on the sequence of the polymer structure. These forms include α , β , and γ chitin, formed by the different arrangement of chains in the crystal region. Alpha chitin is the most abundant and stable form in nature. It is harder than the other forms of chitin [25, 26].

Cydalima perspectalis (Walker) (Lepidoptera: Crambidae) is a boxwood pest that originated in East Asia (China, Japan, and Korea) and is an invasive species in Turkey [27]. This species is known as the boxwood moth and has spread to many parts of Turkey in a short time. It is widespread in boxwood forests, parks, and gardens where Buxaceae plants are found [28]. This invasive moth quickly spread to the entire Black Sea Region, where the Boxwood species is found. Their invasion caused large parts of boxwood areas in boxwood forests in the Eastern Black Sea Region to dry up. For this study, we collected *C. perspectalis* from *Buxus sempervirens* L. trees in the Firtuna Valley of the Meydan Village road in the Çamlıhemşin district of Rize province and the boxwood saplings around the Rize Central exit of the Rize Salarha Tunnel. Many dead *C. perspectalis* moths were obtained during the fight against *C. perspectalis* in this region [29]. It is a great advantage that the dead moths collected after the mechanical struggle are evaluated as biological waste, and these wastes are transformed into a new product, especially chitin. This means a

significant amount of chitin production from many *C. perspectalis* not only for the Eastern Black Sea region but also for the whole country and even the world.

Additionally, because it is easy to collect the larvae and pupae of *C. perspectalis*, obtaining biotechnological products from this moth is convenient. In this study, we characterized the chitin content produced from different forms and body parts of the boxwood pest *C. perspectalis*, which can spread rapidly due to the widespread use of the Buxaceae plant in parks and gardens throughout the world for landscaping. Also, we determined the antimicrobial and cytotoxic effects of the produced chitin.

Materials and methods

Collection of samples

Cydalima perspectalis adults and pupae were collected from *Buxus sempervirens* L. trees in the Firtina Valley of the Meydan Village road in the Çamlıhemşin district of Rize (May to June) (2021) and from the boxwood saplings around the Rize Center exit of the Rize Salarha Tunnel, Recep Tayyip Erdoğan University, Department of Biology. The samples were brought to the Zoology Research Laboratory. Larvae transformed into adults in the laboratory (Fig. 1). The pupal shells of approximately 200 specimens were collected from adults. The wings, body, head, and legs were grouped separately and dried on a plate in an oven at 50 °C for 3–4 days, and the dry weight was recorded separately.

Chitin isolation

For removing the minerals, the chitin samples were prepared with 250 mL of 2 M HCl solution and mixed in the reflux system at 60 °C for four h. The samples were repeatedly filtered using filter paper with distilled water till they had a neutral pH. The minerals were collected from the wings. After demineralization, the protein was



Fig. 1 *Cydalima perspectalis* adults

removed by refluxing the chitin at 50 °C for 20 h using a 2 M NaOH solution. Next, the samples were washed with distilled water till they had a neutral pH and then were dried at 60 °C for 4 h after deproteinization. In the last step, the color was removed. The sample was treated with a mixture of chloroform, methanol, and water (v/v 1:2:4) at room temperature for 1 h. Finally, the samples were dried, and their weights were recorded.

Scanning electron microscopy

To examine the surface morphology of the chitin obtained from the samples, the samples were coated with gold using a Sputter Coater (Cressington Auto 108) brand gold plating device, and then, the chitin samples were photographed using the EVO LS 10 ZEISS microscope.

Fourier-transform infrared spectroscopy

The infrared spectra of the chitin samples of *C. perspectalis* were recorded in the range of 4000–650 cm⁻¹ using the Perkin-Elmer FTIR spectrometer.

Thermogravimetric analysis (TGA)

For the TGA analysis of the chitin obtained from the body parts of *C. perspectalis*, DTG, and TG curves were generated using EXSTAR S11 7300 due to its thermal degradation at a heating rate of 10 °C min⁻¹.

Elemental analysis (EA)

Thermo Flash 2000 was used to determine the *N*, *H*, and *C* contents of the chitin obtained from *C. perspectalis*. The degree of acetylation (DA) of chitin was then calculated using Eq. (1) [30].

$$DA = [(C/N - 5.14)/1.72] \times 100 \quad (1)$$

Evaluation of the antimicrobial effect

The antimicrobial effect of insect chitin samples was determined using *Escherichia coli* ATCC 25922 (Gram-negative), *Bacillus subtilis* (Gram-positive), *Staphylococcus aureus* ATCT 25923 (Gram-positive), and *Candida albicans*, following a modified version of the method described by Chopra [31].

For analyzing the antibacterial activity of chitin, stock cultures of *Escherichia coli*, *Staphylococcus aureus*, *Bacillus subtilis*, and *Candida albicans* showed multidrug resistance and produced a biofilm were incubated at 37 °C for 24 h. The selected bacterial colonies, after incubation, were collected with 5 mL of Mueller–Hinton (MH) broth; the yeast samples were inoculated in the Potato Dextrose Agar (PDA)

culture medium. After shaking for about 18 h at 37 °C, it was diluted in MH broth (1:100) and transferred into 5 mL tubes. The samples of the sterilized chitin were transferred into each tube separately and incubated at 37 °C for 72 h. The chitin samples were removed from the medium and washed with PBS. Then, the samples were incubated in 75% ethanol for about 30 min and left to dry. Finally, bacterial attachment and biofilm formation on chitinous surfaces were examined by SEM.

Cell cytotoxicity assay

We obtained L929 (mouse fibroblast) cells from LAW, Sap Institute (Ankara, Turkey). The cells were grown in Dulbecco's modified Eagle's medium (DMEM) containing a 10% solution of fetal bovine serum (FBS), penicillin (100 units/mL), and streptomycin (100 µg/mL). For the MTT analysis, the density of the cells was adjusted to 1×10^4 cells/mL per well and seeded in 96-well culture plates. The plates were incubated for 24 h at 37 °C in 5% CO₂. After 24 h, pre-sterilized samples were added to each well, and the cultures were incubated under the previously specified conditions for 24, 48, and 72 h without changing the medium. The untreated control cells were maintained for the exact durations to compare growth inhibition. The cytotoxicity of the samples to the cells was evaluated by performing the MTT assay.

The samples were removed from the wells after incubation, and then, the MTT solution (0.5 mg mL⁻¹) was added to all test and control wells. The plates were incubated at 37 °C for three h in the dark. Then, the reaction mixture was removed from the wells, and 100 µL of DMSO solution was added to dissolve the formazan crystals. It was left for 5 min to stabilize the color, and then, the absorbance was measured at 492 nm using the Chromate®ELISA reader. The viability of untreated cells in the sample's absence was considered 100%. Cell viability percentage (%) was calculated using Eq. (2).

$$\% \text{ Vitality} = ((\text{Abs}_{\text{sample}} - \text{Abs}_{\text{blank}}) / (\text{Abs}_{\text{control}} - \text{Abs}_{\text{blank}})) \times 100 \quad (2)$$

The data were analyzed using the GraphPad Prism software (version 5; GraphPad Software®). The data were reported as the mean ± standard error of the mean (SEM) and analyzed by performing one-way ANOVA followed by Tukey's post hoc tests (95% confidence interval). All differences were considered to be statistically significant at $p < 0.05$.

Results and discussion

Scanning electron microscopy

The surface morphology of the chitin samples obtained from five different body regions was visualized by SEM, and five different surface morphologies were observed. In general, all chitinous surfaces were composed of fine nanofibers and porous structures (Fig. 2). However, different chitinous surfaces were formed by the arrangement, pitting, folding, and bending of the nanofibers. In the head, randomly

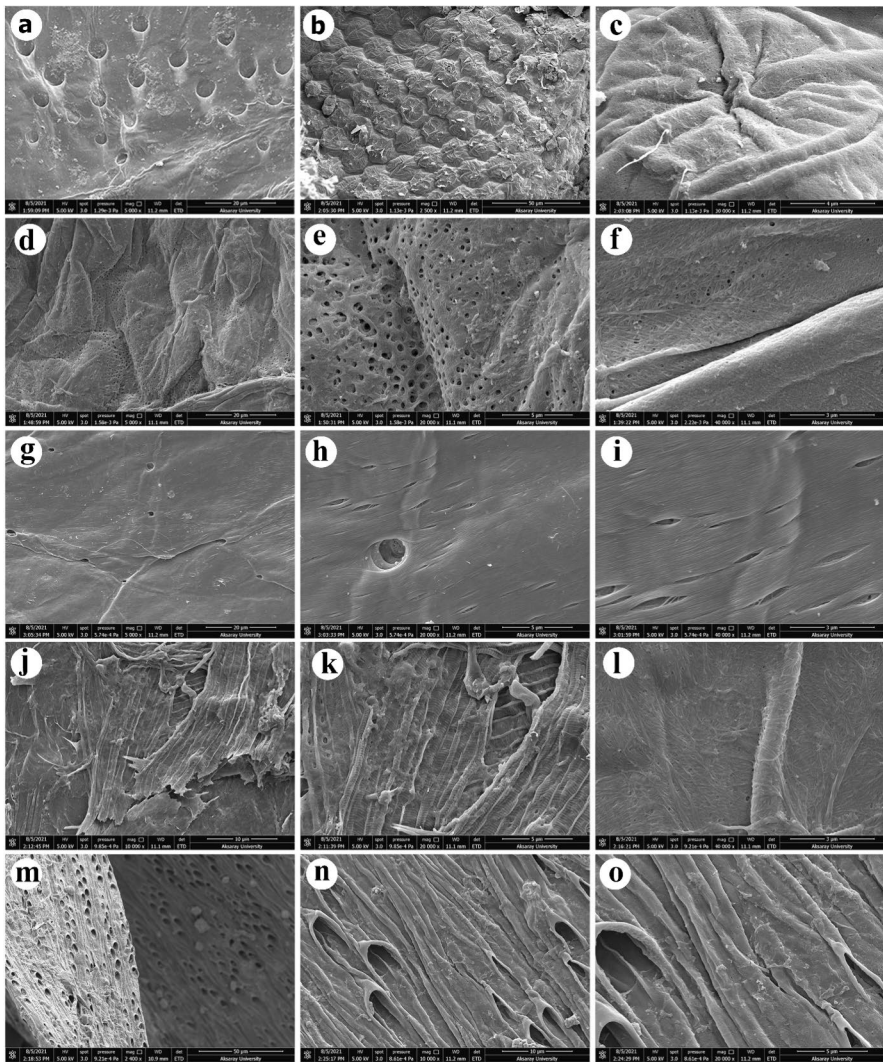


Fig. 2 SEM images of surface morphologies of different chitins obtained from adults of *C. perspectalis*: head area chitin (**a, b, c**); pupa Shell area chitin (**d, e, f**); body area chitin (**g, h, i**); wing area chitin (**j, k, l**); leg area chitin (**m, n, o**)

scattered pits resembling craters were present (Fig. 2a). The chitinous surface of the compound eyes was more curved in the head region, and the typical hexagonal structures of ommatidia were preserved (Fig. 2b and c). The surface of the pupal cover had a wavy appearance and consisted of nanofibers with few and dense micropores (Fig. 2d, e, and f). The chitinous surface of the body (Fig. 2g, h, and i) was flat with simple nanofibers consisting of tight tissues stacked on top of each other and occasional small pores. Longitudinal and transverse venations were visible in the chitin framework of the wings (Fig. 2j, k, and l). There were micropores in a

single row between the veins. The micropores of the chitinous surfaces from the legs (Fig. 2m, n, and o) were grouped, frequent, and prominent. They looked like canals that protruded outward and extended deep. In all surface morphologies, randomly distributed nanopores had a similar structure in high-magnification SEM images ($\times 20,000$, $\times 30,000$, and $\times 40,000$).

Some studies have found that chitin samples from crustaceans and some insects have nanofibers and nanopores [32, 33]. Some chitinous surfaces contain only non-porous nanofibers, while others contain porous nanofibers [12]. We found significant differences in the surface morphologies of the isolated chitin. Many micropores and nanopores were present on the chitinous surfaces, and the surfaces were generally rough and consisted of different pore structures. The chitinous surface of the main body of the moth was flatter, with fewer pores than the surface of the other body parts. The cuticle morphology in arthropods differs between species [34] and between body parts within species. We also found differences in the surface morphologies of chitin from different parts of the body. Thus, there is no standard surface morphology for alpha chitin. The area of use of chitin obtained from *C. perspectalis* was quite different due to surface differences. For the nanofiber, nanopore, and micropore structures and surface patterns of chitin and its derivatives, the chitin samples with different morphological structures might be effective in various biomedical applications. For example, the regular projections of butterfly wings have a structure suitable for cell attachment [35], which increases the biocompatibility of well-produced wing chitin. Chitin-derived scaffolds are widely used because they are renewable, biodegradable, biocompatible, and only slightly toxic [36].

Fourier-transform infrared spectroscopy

The FTIR spectra of the chitin samples obtained from different body parts of *C. perspectalis* in our study are presented in Fig. 3. The most prominent peaks of chitins are mentioned below. For chitin from the wings: 1008, 1155, 1310, 1376, 1553,

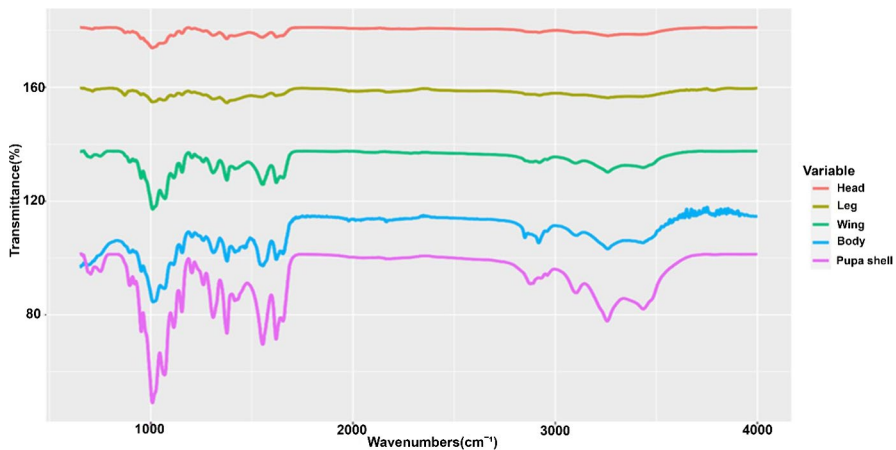


Fig. 3 IR spectra for alpha chitins from five part of *C. perspectalis*

1622, 1654, 2922, 3101, 3260, and 3430 cm^{-1} ; for chitin from the head: 1008, 1154, 1308, 1375, 1549, 1622, 1654, 2875, 2923, 3107, 3259, and 3430 cm^{-1} ; for chitin from the body: 1012, 1062, 1112, 1154, 1310, 1377, 1555, 1620, 1654, 2918, 2958, 3102, 3260, and 3435 cm^{-1} ; for chitin from the pupal shell: 1008, 1069, 1114, 1154, 1308, 1376, 1553, 1620, 1654, 2916, 2961, 3105, 3257, and 3436 cm^{-1} ; for chitin from the legs: 1008, 1070, 1112, 1154, 1311, 1378, 1549, 1619, 1653, 2922, 2957, 3109, 3261, and 3436 cm^{-1} .

The FTIR chemical analysis of the chitin provided insights into its structure and current functions. Chitin can be found in the exoskeleton of insects as α , β , and γ chitin [37]. Alpha chitin has specific characteristic peaks, which occur in the FTIR spectra of chitin samples as distinct absorption bands of some functional groups. These appear as amide I, amide II, and amide III bands [37]. The characteristic feature of the amide I band is its separation into two bands at approximately 1650 and 1620 cm^{-1} [19]. In our study, the FTIR spectra of the chitin samples obtained from the different body parts of *C. perspectalis* are presented in Fig. 3. The results of the FTIR analysis showed that the cuticle of these insects has crystalline alpha chitin. The amide bands of the chitin samples and the molecular movements of these bands are shown in Table 1. For the whole chitin samples, the peaks at 1653 and 1620 cm^{-1} were attributed to the C=O stretch (amide I), while the band at 1551 cm^{-1} was attributed to NH bending (amide II). We found bands of C–N stretching at 1,311 cm^{-1} and C–H bending at 1376 cm^{-1} (amide III). The bands obtained by the FTIR analysis were similar in all chitin samples. Additionally, the FTIR bands of the chitin samples in this study were similar to the FTIR bands of alpha chitin isolated from different organisms in other studies [12].

Thermogravimetric analysis

Thermal stability is a property that ensures the decomposition of the structures in the materials during heating [38]. Thermogravimetric analysis is a technique that quantitatively gives the change in the mass of the material depending on the increasing temperature [39]. Thermogravimetric analysis was performed to check the thermal stability and degradation sequence of the chitin samples obtained from adult *C. perspectalis*. The thermograms of these samples are shown in Fig. 4. According

Table 1 Stresses and vibrations in the Amid I, Amid II and Amid III bands of chitins obtained from the leg, head, wing, body and pupa shell of *C. perspectalis*

Region	Wavelength peaks (cm^{-1})					Molecular Motion
	Leg	Head	Wing	Body	Pupa shell	
Amid I	1653	1653	1654	1654	1654	C=O secondary stretch
	1619	1621	1621	1620	1620	C=O secondary stretch
Amid II	1549	1549	1553	1550	1553	N–H bend, C–N stretch
Amid III	1311	1308	1308	1310	1308	C–N stretch
	1378	1375	1376	1378	1376	C–H bending vibrations

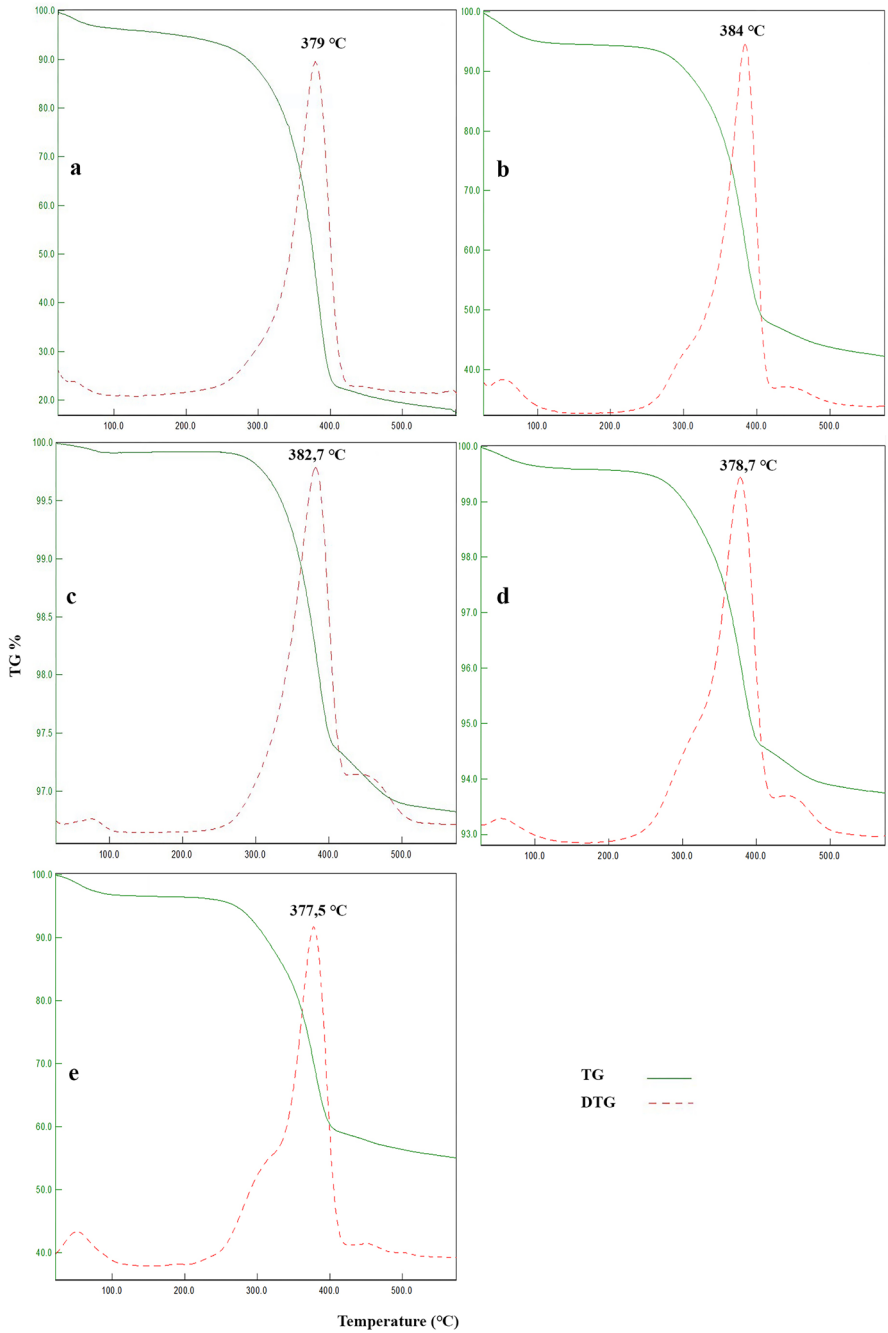


Fig. 4 TGA and DTG thermo-grams for chitin isolated from *Cydalima perspectalis* adults: **a** head, **b** leg, **c** wings, **d** body and **e** pupal shell

to the results, it was observed that the mass losses of chitins occurred in two main stages. Thermograms showed that the first mass loss occurred at about 100 °C and the second at 150–600 °C. The initial loss at 0–150 °C may be due to removing water adsorbed to the chitin molecules [40]. The percentage mass loss in the second stage from different body parts was as follows: wing: 6%, head: 42%, pupal shell: 52%, body: 3%, and leg: 78% (Fig. 4). The maximum decomposition temperatures (DTGmax) of the chitin samples obtained from the head, body, legs, wings, and pupal shell were 374.4, 382.6, 379, 379.1, and 382.3 °C, respectively. The second loss at 150–600 °C was associated with the acetylated and deacetylated units of chitin and the degradation of the polysaccharide structure of the molecule [41]. Also, the DTGmax values of the chitin samples were similar to those of the commercial chitin (386 °C).

According to the present results, the secondary mass loss in the wings and body was lower than in the head, legs, and pupal shells. Additionally, the chitin obtained from the head had the lowest thermal stability (DTG max: 377.5 °C), while the chitin obtained from the pupal shells exhibited the highest thermal stability (DTG max: 384 °C). The DTGmax values (375 °C and 382 °C) of chitin samples obtained from different animals (e.g., crabs and insects) in previous studies, as determined by TGA, were similar to the DTGmax values recorded in our study [42, 43].

DTG data for alpha chitin in the literature range from 355° to 395° [38, 44–46]. In conclusion, the TG diagrams of the chitin samples obtained from *C. perspectalis* were similar to those found in studies on α -chitin.

In some chitins, a third thermal decomposition was observed after 600 °C. It is thought that this difference is due to the rearrangement of chemical bonds at higher temperatures [21]. A similar situation was observed in our study (pupal shell, leg, and body).

Elemental analysis (EA)

The C, N, H, and DA values of the content of the chitin samples obtained from *C. perspectalis* are shown in Tab. 2. The nitrogen element percents were determined as 6.3, 6.4, 6.7, 2.66, and 6.9 for wing, body, leg, head, and pupa shell, respectively, in this study.

Chitin has the highest natural nitrogen content in the world after protein [47]. The N percentage values in the content of the chitin were found to be 5.92% in wasps,

Table 2 The C, N, H and DA values of the content of chitins obtained from *C. perspectalis*

Region	Content (%)				
	<i>N</i>	<i>C</i>	<i>H</i>	<i>C/N</i>	DA
Wing	6.31	45.64	18.57	7.23	122
Body	6.44	48.86	7.67	7.58	142
Leg	6.68	47.43	7.04	7.10	114
Head	2.66	28.48	3.45	10.70	323
Pupa shell	6.93	44.49	7.67	6.41	74

6.45% in *Holotrichia parallela* (insect), 5.92% in cicadas [19, 33, 42, 48], and 6.89% in pure chitin. When the N atom content of the isolated chitins in this study was compared with the literature data (except for the head chitin), the values were similar to the literature. The nitrogen content for pure chitin was determined as 6.89%. If the N content of chitin is more than 6.89%, protein structures are still in the structure; if less than 6.89% [19], inorganic structures are still in the structure [49]. The pupal shell had the highest chitin percentage (6.9%), and the lowest was the head chitin (2.66%). In addition, the impurity in the chitin also affects the percentages of N and C values in the structure [50]. The carbon atom percent of extracted α -chitin from species in literature was determined as 39.2–49.0% [21, 34, 51]. According to earlier reports, C/N values calculated from the elemental analysis are between 8.5% and 8.5 [21]. However, in our study, this value varies from 8 to 6. The DA should not exceed 100% in well-purified chitin [51]. In our study, except for the pupal shell, this value was higher than the theoretical value for the examined chitins. This indicates that mineral residues in the chitin structure could not be completely removed. In previous studies, DA values were determined as 250 and 179 for larvae and adults of *H. illucens* [51], 108% and 232% for adult potato beetle [52], and 212, 212, 218, and 195% for *Bradyporus (Callimenus) sureyai*, *Gryllotalpa gryllotalpa*, *Polyphylla fullo*, *Lucanus cervus* species [21]. As a result, all these data show the presence of some inorganic materials in the structure of chitins.

Antimicrobial assay

The attachment of *Escherichia coli*, *Staphylococcus aureus*, *Bacillus subtilis*, and *Candida albicans* on the chitinous surfaces obtained from *C. perspectalis* and the formation of a biofilm on these surfaces were examined by SEM. The growth stages, including multiple biofilm clusters and the colonization and formation of the polysaccharide matrix on different chitinous surfaces, are shown in Fig. 5. Chitin surfaces have a heterogeneous and rough surface, and chitins differ from each other due to their surface morphology. The surfaces were coated with polymeric substances in a layer after the microorganisms adhered to the surface. After 72 h of biofilm formation, a few specialized structures similar to honeycomb and wall, channels, and mushroom-like structures with pronounced cellular growth were seen. As a result, a dense and irregular layer was formed by the extracellular structure within the polymer structure secreted by microorganisms. This was especially prominent in the biofilm layer formed by *E. coli* on the chitinous surfaces of the body, legs, and wings. The microorganisms were generally embedded in the polymer matrix (Fig. 5x, j, and n). The chitinous surfaces of the wings and legs were colonized the most because these surfaces have many holes, channels, and layers that provide suitable conditions for the reproduction of these microorganisms. The least colonization occurred on the chitinous surfaces of pupae (Fig. 5r, s, t, and u). As a result, the biofilms adhered well to the irregular chitinous surfaces. The use of SEM in this study is to demonstrate that different microorganisms can form diverse biofilm structures on chitins.

It has been shown in previous studies that substrate surfaces are adequate for the adhesion and growth of microorganisms in the formation of biofilms [53,

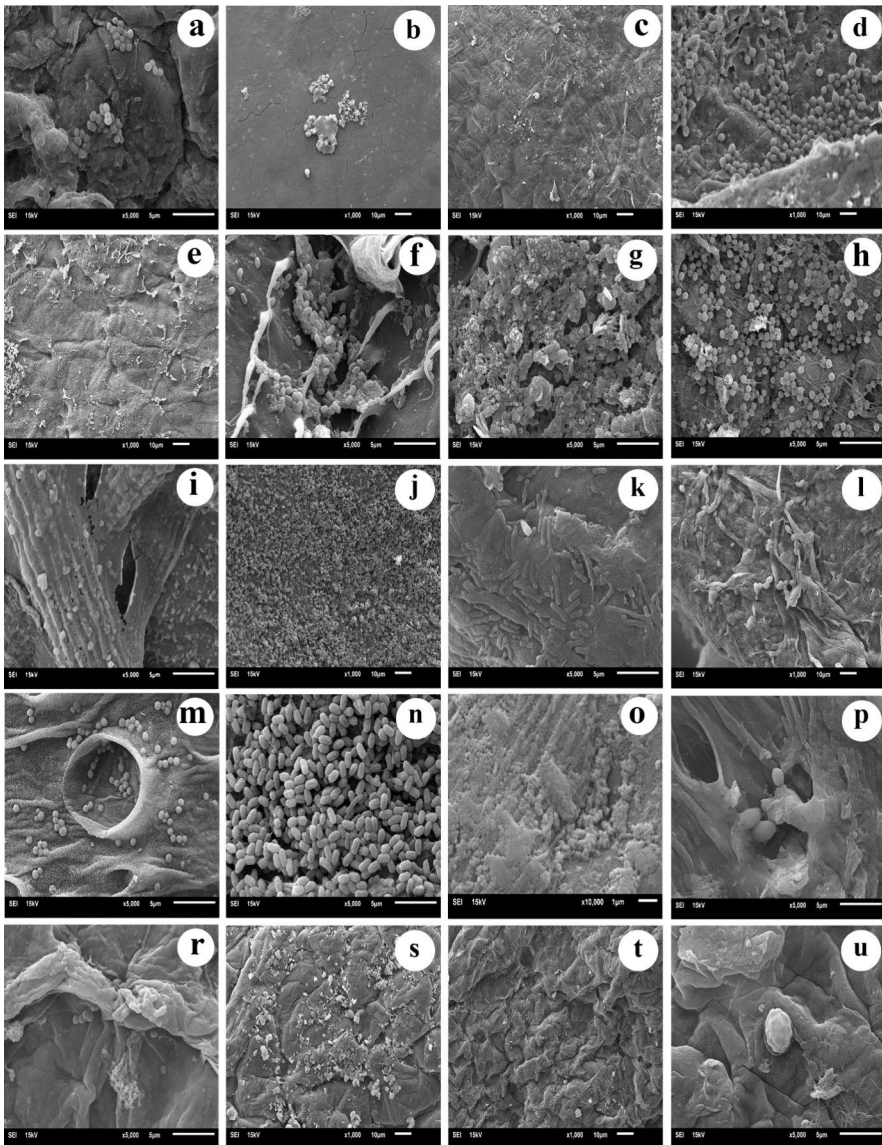


Fig. 5 SEM images of *Escherichia coli*, *Bacillus subtilis*, *Staphylococcus aureus* and *Candida albicans* biofilms formed on different chitin surfaces isolated from *Cydalima perspectalis*: **a** head-*S.aureus*, **b** head-*B.subtilis*, **c** head-*E.coli*, **d** head-*C. albicans*, **e** body-*S.aureus*, **f** body-*B.subtilis*, **g** body-*E.coli*, **h** body-*C. albicans*, **i** wing-*S.aureus*, **j** wing-*B.subtilis*, **k** wing-*E.coli*, **l** wing-*C. albicans*, **m** leg-*S.aureus*, **n** leg-*B.subtilis*, **o** leg-*E.coli*, **p** leg-*C. albicans*, **r** pupa shell-*S.aureus*, **s** pupa shell-*B.subtilis*, **t** pupa shell-*E.coli* ve, **u** pupa shell-*C. albicans*

54]. There are many studies on biofilm formation on chitin surfaces. Some of the microorganisms used in these studies are: *Vibrio cholerae* [54], *Salmonella* sp. [55], *Staphylococcus aureus* [56], and *Proteus mirabilis* [57]. The physical or

chemical treatment of chitin affects biofilm formation [58]. We conclude that the moth's original chitin surfaces have a microbial property and that microorganisms often form a film on the surface. Recently, biofilms have been used as therapeutic biomaterials in various fields. It is used in tissue culture, wound treatment [59] and in the field of bioremediation for water purification [60]. In this study, we concluded that chitin substrates can be used for biofilm production. Biofilm production can be prevented by coating the organic material surfaces with silver, so that the organic surface gains antimicrobial properties [61].

Cell cytotoxicity assay (MTT)

In the MTT assay, the viability of cells is proportional to the activity of the mitochondrial dehydrogenase enzyme. Formazan crystals are formed due to the mitochondrial activity in living cells. When these formazan crystals dissolve in solvents such as DMSO, they form a purple color, whose intensity is proportional to cell viability. The results of the MTT assay were measured at 492 nm using a microplate reader (ChroMate®ELISA).

The MTT analysis was performed at 24, 48, and 72 h for the relevant biomaterials. This analysis selected the cells without any material containing only DMEM as the control group. The percentage cell viability of the materials relative to the control group for 24, 48, and 72 h is shown in Fig. 5. The results (MTT results) for cell viability showed that the samples (2 mm in diameter) had no cytotoxic effects on the L929 cells at 24, 48, and 72 h (all values > ~70%). The difference in vitality (%) between legs and body, head and body, and body and shell for 24 h was statistically significant (*,**; $p < 0.05$). However, the vitality (%) difference between samples at the 48th hour was insignificant. The vitality level of the shell sample at 72 h was significantly lower than that of the control (*; $p < 0.05$). The level of statistical significance between groups is shown in the graphs (Fig. 6). The results of the MTT assay showed that the chitin did not produce other cytotoxic substances and was safe for cell culture. Other studies reported similar results with other chitin derivatives [62]. It was observed that cell viability increased depending on the incubation period of chitin/fibroin and alpha chitin on HFFF2 cells [63]. The biocompatibility of chitin was evaluated in an in vivo study for bone regeneration following treatment with chitin HA [64]. In another study, chitin isolates obtained from shrimp shells and the mycelium of mushrooms did not show significant cytotoxicity in mice, human fibroblasts, and osteoblasts [65]. The biochemical roles of chitin and its deacetylated forms in wound healing include fibroblast activation, polymorphonuclear cell activation, cytokine production, giant cell migration, and stimulation of type IV collagen synthesis [66]. It has been stated that chitin nanogels may be a good alternative as a cancer therapeutic agent [67], and it has also attracted attention due to its biological activity and sensitivity to degradation by enzymes found in body fluids such as lysozyme and *N*-acetylglucosaminidase [68]. Overall, chitin is a biopolymer that accelerates wound healing.

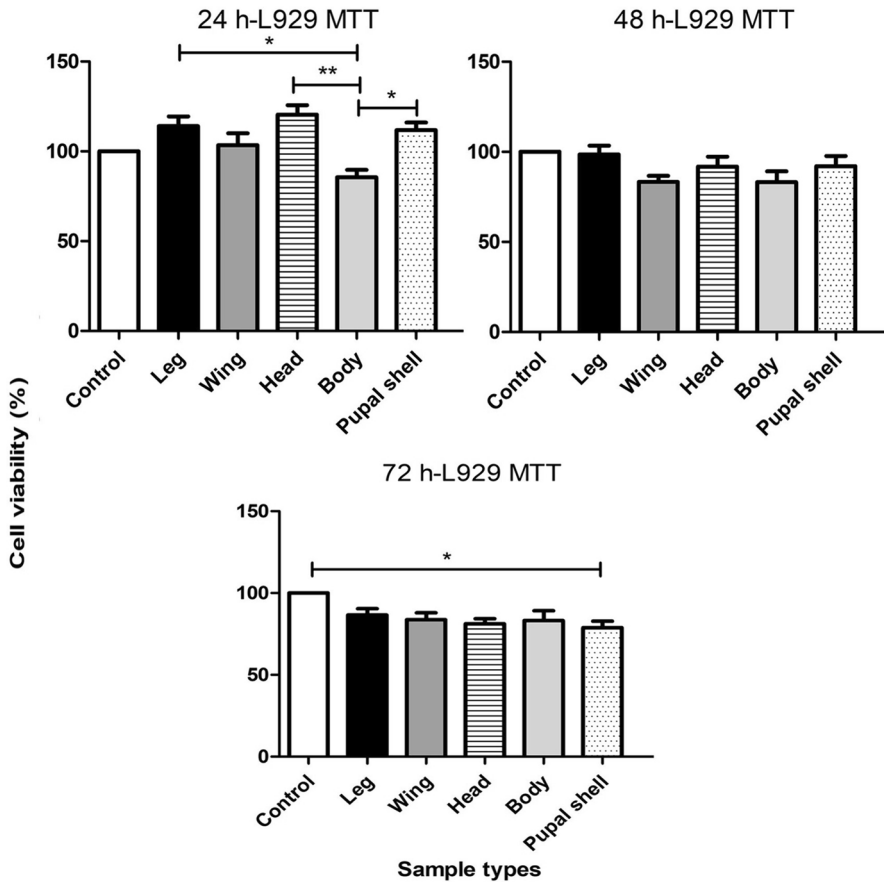


Fig. 6 Graphs of percent cell viability of chitins from the leg, head, wing, body, and pupal shell of *C. perspectalis* compared to the control group at 24, 48, and 72 h

Conclusion

In the present study, we investigated the physicochemical properties and the cytotoxic and antimicrobial effects of different chitin samples obtained from adult *C. perspectalis* moths. We also determined the chitin content and the cytotoxic and antimicrobial effects of *C. perspectalis*. The FTIR, TGA, SEM, and elemental analyses showed that the samples had α -chitin, which is specific to insect chitin. The bands obtained in the FTIR analysis were similar in all chitin samples. The thermal stability and decomposition rates of the chitin samples were very similar. The SEM images showed that the surface morphologies of the chitin samples were different from each other. The results of the MTT assay showed that chitin had a cytotoxic effect on L929 cells. Additionally, different microorganisms formed a biofilm on chitin surfaces. These chitin samples can be used for cell adhesion, specific surface area generation, high porosity, and biocompatibility,

especially in tissue engineering. It is also an alternative product for biofilm production.

Acknowledgements This manuscript is based on Doctorate Thesis (Recep Tayyip Erdoğan University). The authors thank Prof. Dr. Murat Kaya for his contribution. Furthermore, it was presented as an oral presentation at the 1st International Boxwood Workshop, Recep Tayyip Erdoğan University, Rize, Turkey, 25–27 October 2021, and it was published as a summary abstract in the proceedings book.

Funding Open access funding provided by the Scientific and Technological Research Council of Türkiye (TÜBİTAK). This study was supported by the Research Fund of the Recep Tayyip Erdoğan University, Project Number: FDK-2022-1319.

Declarations

Conflict of interest The authors declare that they have no conflict of interest.

Ethical approval and consent to participate Not applicable.

Open Access This article is licensed under a Creative Commons Attribution 4.0 International License, which permits use, sharing, adaptation, distribution and reproduction in any medium or format, as long as you give appropriate credit to the original author(s) and the source, provide a link to the Creative Commons licence, and indicate if changes were made. The images or other third party material in this article are included in the article's Creative Commons licence, unless indicated otherwise in a credit line to the material. If material is not included in the article's Creative Commons licence and your intended use is not permitted by statutory regulation or exceeds the permitted use, you will need to obtain permission directly from the copyright holder. To view a copy of this licence, visit <http://creativecommons.org/licenses/by/4.0/>.

References

1. Üçgül İ, Sultan A, Özdemir Küçükçapraz D (2016) Purification of kit from different raw material sources and textile applications. *Erzincan Univ J Sci Technol* 9(1):46–56
2. Muzzarelli RAA (1996) Chitosan-based dietary foods. *Carbohydr Polym* 29(4):179–197
3. Ehrlich H, Kaluzhnaya OV, Brunner E et al (2013) Identification and first insights into the structure and biosynthesis of chitin from the freshwater sponge *Spongilla lacustris*. *J Struct Biol* 183(3):474–483
4. Wysokowski M, Bazhenov VV, Tsurkan MV et al (2013) Isolation and identification of chitin in three-dimensional skeleton of *Aplysina fistularis* marine sponge. *Int J Biol Macromol* 62:94–100
5. Bo M, Bavestrello G, Kurek D et al (2012) Isolation and identification of chitin in the black coral *Parantipathes larix* (Anthozoa: Cnidaria). *Int J Biol Macromol* 51(1–2):129–137
6. Jalal AF, Risheed CM, Ibrahim BM (2012) Optimization of chitin extraction from chicken feet. *J Anal Bioanal Tech* 3(5)
7. Gonil P, Sajomsang W (2012) Applications of magnetic resonance spectroscopy to chitin from insect cuticles. *Int J Biol Macromol* 51(4):514–522
8. Badaway RM, Mohamed HI (2015) Chitin extraction, composition of different six insect species and their comparable characteristics with that of the shrimp. *J Am Sci* 11(6):127–134
9. Mohan K, Ganesan AR, Muralisankar T et al (2020) Recent insights into the extraction, characterization, and bioactivities of chitin and chitosan from insects. *Trends Food Sci Technol* 105:17–42
10. Nickerl J, Tsurkan M, Hensel R, Neinhuis C, Werner C (2014) The multi-layered protective cuticle of *Collembola*: a chemical analysis. *J R Soc Interface* 11(99):20140619
11. Özpırlak H (2003) The structure of the cuticle in insects, molting and the effects of diflubenzuron (DFB). *Selcuk Univ Faculty Sci J Sci* 1(21):7–20

12. Kaya M, Baran T, Erdoğan S et al (2014) Physicochemical comparison of chitin and chitosan obtained from larvae and adult *Colorado potato beetle* (*Leptinotarsa decemlineata*). *Mater Sci Eng* 45:72–81
13. Senevirathne M, Ahn CB, Kim SK, Je JY (2011) Cosmeceutical applications of chitosan and its derivatives. In: *Marine cosmeceuticals: trends and prospects*, p. 169
14. Jayakumar R, Prabakaran M, Nair SV, Tamura H (2010) Novel chitin and chitosan nanofibers in biomedical applications. *Biotechnol Adv* 28(1):142–150
15. Kaya M, Sargin I, Al-Jaf I, Erdogan S, Arslan G (2016) Characteristics of corneal lens chitin in dragonfly compound eyes. *Int J Biol Macromol* 89:54–61
16. Kim MW, Han YS, Jo YH et al (2016) Extraction of chitin and chitosan from housefly, *Musca domestica*, pupa shells. *Entomol Res* 46(5):324–328
17. Kaya M, Baublys V, Can E et al (2014) Comparison of physicochemical properties of chitins isolated from an insect (*Melolontha melolontha*) and a crustacean species (*Oniscus asellus*). *Zoomorphology* 133:285–293
18. Kaya M, Baran T, Ozusaglam MA et al (2015) Extraction and characterization of chitin and chitosan with antimicrobial and antioxidant activities from cosmopolitan *Orthoptera species* (Insecta). *Biotechnol Bioprocess Eng* 20:168–179
19. Liu S, Sun J, Yu L et al (2012) Extraction and characterization of chitin from the beetle *Holotrichia parallela* motschulsky. *Molecules* 17(4):4604–4611
20. Majtan J, Bilikova K, Markovic O, Grof J, Kogan G, Simuth J (2007) Isolation and characterization of chitin from bumblebee (*Bombus terrestris*). *Int J Bio Macromol* 40(3):237–241
21. Kabalak M, Aracagök D, Torun M (2020) Extraction, characterization and comparison of chitins from large bodied four Coleoptera and Orthoptera species. *Int J Biol Macromol* 145:402–409
22. Kaya M, Bitim B, Mujtaba M, Koyuncu T (2015) Surface morphology of chitin highly related with the isolated body part of butterfly (*Argynnis pandora*). *Int J Biol Macromol* 81:443–449
23. Waško A, Bulak P, Polak-Berecka M, Nowak K, Polakowski C, Bieganski A (2016) The first report of the physicochemical structure of chitin isolated from *Hermetia illucens*. *Int J Biol Macromol* 92:316–320
24. Kaya M, Sofi K, Sargin I, Mujtaba M (2016) Changes in physicochemical properties of chitin at developmental stages (larvae, pupa and adult) of *Vespa crabro* (wasp). *Carbohydr Polym* 145:64–70
25. Minke R, Blackwell J (1978) The structure of α -chitin. *J Mol Biol* 120(2):167–181
26. Kurita K (1998) Chemistry and application of chitin and chitosan. *Polym Degrad Stab* 59(1–3):117–120
27. Öztürk N, Akbulut S, Yüksel B (2016) A new pest *Cydalima perspectalis* (Walker, 1859) (Lepidoptera: Crambidae) For Düzce. *Düzce Univ For Faculty J For* 12(1):112–121
28. Hizal E, Kose M, Yesil C, Kaynar D (2012) The new pest *Cydalima perspectalis* (Walker, 1859) (Lepidoptera: Crambidae) in Turkey. *J Anim Vet Adv* 11(3):400–403
29. Aksu Y, Göktürk ÇB, Aksu G (2021) Damage, biology and control studies of *Cydalima perspectalis* Walker, 1859 (Lepidoptera: Crambidae) damages in *Buxus sempervirens* Forests. *J For Hunt* 3:29–36
30. Al Sagheer FA, Al-Sughayer MA, Muslim S, Elsabee MZ (2009) Extraction and characterization of chitin and chitosan from marine sources in Arabian Gulf. *Carbohydr Polym* 77(2):410–419
31. Chopra V, Thomas J, Sharma A et al (2021) A bioinspired, ice-templated multifunctional 3D cryogel composite crosslinked through in situ reduction of GO displayed improved mechanical, osteogenic and antimicrobial properties. *Mater Sci Eng C* 119:111584
32. Mushi NE, Butchosa N, Salajkova M et al (2014) Nanostructured membranes based on native chitin nanofibers prepared by mild process. *Carbohydr Polym* 112:255–263
33. Yen MT, Yang JH, Mau JL (2009) Physicochemical characterization of chitin and chitosan from crab shells. *Carbohydr Polym* 75(1):15–21
34. Kaya M, Erdogan S, Mol A, Baran T (2015) Comparison of chitin structures isolated from seven Orthoptera species. *Int J Biol Macromol* 72:97–805
35. Kholghi-Eshkalak L, Jalali Sendi J, Karimi-Malati A, Zibae A (2017) Life table parameters and biological characteristics of citrus butterfly *Papilio demoleus* (Lepidoptera: Papilionidae) on various citrus hosts. *J Crop Prot* 6(3):15–325
36. Casadidio C, Peregrina D, Gigliobianco M et al (2019) Chitin and chitosans: characteristics, eco-friendly processes, and applications in cosmetic science. *Mar Drugs* 17(6):369

37. Shushizadeh MR, Pour EM, Zare A, Lashkari Z (2015) Persian gulf β -chitin extraction from sepia pharaonis sp. cuttlebone and preparation of its derivatives. *Bioactive Carbohydrates Dietary Fibre* 6(2):133–142
38. Muzzarelli RA, Morganti P, Morganti G, Palombo P, Palombo M, Biagini G, Muzzarelli C (2007) Chitin nanofibrils/chitosan glycolate composites as wound medicaments. *Carbohyd Polym* 70(3):274–284
39. Bischof JC, He X (2006) Thermal stability of proteins. *Ann New York Acad Sci* 1066(1):12–33. <https://doi.org/10.1196/annals.1363.003>
40. Ifuku S, Nogi M, Yoshioka M et al (2010) Fibrillation of dried chitin into 10–20 nm nanofibers by a simple grinding method under acidic conditions. *Carbohyd Polym* 81(1):134–139
41. Juárez-de La Rosa BA, Quintana P, Yáñez-Limón JM, Alvarado-Gil JJ (2012) Effects of thermal treatments on the structure of two black coral species chitinous exoskeleton. *J Mater Sci* 47:990–998
42. Sajomsang W, Gonil P (2010) Preparation and characterization of α -chitin from *Cicada sloughs*. *Mater Sci Eng C* 30(3):357–363
43. Kaya M, Sargin I, Tozak KÖ et al (2013) Chitin extraction and characterization from *Daphnia magna* resting eggs. *Int J Biol Macromol* 61:459–464
44. Paulino AT, Siminato JI, Carcia JC, Nozaki J (2006) Characterization of chitosan and chitin produced from silk worm chrysalides. *Carbohyd Polym* 64(1):98–103
45. Al-Sagheer FA, Al-Sughayer MA, Muslim MZ, Elsabee S (2009) Extraction and characterization of chitin and chitosan from marine sources in Arabian gulf. *Carbohyd Polym* 77(2):410–419
46. Sajomsang W, Gonil P (2010) Preparation and characterization of α -chitin from cicada sloughs. *Mater Sci Eng C* 30(3):357–363
47. de Britto D, Celi Goy R, Campana SP et al (2011) Quaternary salts of chitosan: history, antimicrobial features, and prospects. *Int J Carbohydrate Chem* 2011:1–12
48. Majtán J, Břiliková K, Markovič O et al (2007) Isolation and characterization of chitin from bumblebee (*Bombus terrestris*). *Int J Biol Macromol* 40(3):237–241
49. El Knidri HE, Belaabed R, El Khalfaouy R et al (2017) Physicochemical characterization of chitin and chitosan Produced from *Parapenaeus longirostris* shrimp Shell wastes. *J Mater Environ Sci* 8(10):3648–3653
50. Yen MT, Mau JLP (2007) Physico-chemical characterization of fungal chitosan from shii-take stipes. *LWT-Food Sci Technol* 40(3):472–479
51. Waško A, Bulak P, Polak-Berecka M et al (2016) The first report of the physicochemical structure of chitin isolated from *Hermetia illucens*. *Int J Biol Macromol* 92:316–320
52. Kaya M, Baran T, Erdoğan S et al (2014) Physicochemical comparison of chitin and chitosan obtained from larvae and adult *Colorado potato beetle* (*Leptinotarsa decemlineata*). *Mater Sci Eng C* 45:72–81
53. Azeredo J, Azevedo NF, Briandet R et al (2017) Critical review on biofilm methods. *Crit Rev Microbiol* 43(3):313–351
54. Pruzzo C, Vezzulli L, Colwell RR (2008) Global impact of *Vibrio cholerae* interactions with chitin. *Environ Microbiol* 10(6):1400–1410
55. Brandl MT, Carter MQ, Parker CT et al (2011) Salmonella biofilm formation on *Aspergillus niger* involves cellulose–chitin interactions. *PLoS ONE* 6(10):e25553
56. Banerjee S, Saha A, Dutta S et al (2015) Effect of different antibiotics against in vitro *Staphylococcus aureus* biofilm grown on chitin flakes. *South Asian J Exp Biol* 5(1):22–25
57. Fernández-Delgado M, Duque Z, Rojas H et al (2015) Environmental scanning electron microscopy analysis of *Proteus mirabilis* biofilms grown on chitin and stainless steel. *Ann Microbiol* 65(3):1401–1409
58. Salaberria AM, Fernandes SC, Diaz RH, Labidi J (2015) Processing of α -chitin nanofibers by dynamic high pressure homogenization: characterization and antifungal activity against *A. niger*. *Carbohyd Polym* 116:286–291
59. Picheth GF, Pirich CL, Sierakowski MR et al (2017) Bacterial cellulose in biomedical applications: a review. *Int J Biol Macromol* 104:97–106
60. Aranaz I, Mengfbar M, Harris R et al (2009) Functional characterization of chitin and chitosan. *Curr Chem Biol* 3(2):203–230
61. Zang LS, Chen YM, Koc-Bilican B et al (2021) From bio-waste to biomaterials: the eggshells of Chinese oak silkworm as templates for SERS-active surfaces. *Chem Eng J* 426:131874

62. Je JY, Kim SK (2006) Antioxidant activity of novel chitin derivative. *Bioorg Med Chem Lett* 16(7):1884–2188
63. Mehrabani MG, Karimian R, Rakhshaei R et al (2018) Chitin/silk fibroin/TiO₂ bio-nanocomposite as a biocompatible wound dressing bandage with strong antimicrobial activity. *Int J Biol Macromol* 116:966–976
64. Ge Z, Baguenard S, Lim LY, Wee A, Khor E (2004) Hydroxyapatite–chitin materials as potential tissue engineered bone substitutes. *Biomaterials* 25(6):1049–1058
65. Teng WL, Khor E, Tan TK, Lim LY, Tan SC (2001) Concurrent production of chitin from shrimp shells and fungi. *Carbohyd Res* 332(3):305–316
66. Mezzana P (2008) Clinical efficacy of a new chitin nanofibrils-based gel in wound healing. *Acta Chir Plast* 50(3):81–84
67. Jayakumar R, Nair A, Rejinold NS, Maya S, Nair SV (2012) Doxorubicin-loaded pH-responsive chitin nanogels for drug delivery to cancer cells. *Carbohyd Polym* 87(3):2352–2356
68. Muzzarelli RA (1993) Biochemical significance of exogenous chitins and chitosans in animals and patients. *Carbohyd Polym* 20(1):7–16

Publisher's Note Springer Nature remains neutral with regard to jurisdictional claims in published maps and institutional affiliations.